# Quantum criticality and superconducting pairing in $Ce_{1-x}Yb_xCoIn_5$ alloys

**Y P Singh,**[1] **D J Haney,**[1] **I K Lum,**[2] **B D White,**[2] **M B Maple,**[2] **M Dzero,**[1] **and C C Almasan**[1]

[1]Department of Physics, Kent State University, Kent, Ohio, 44242, USA,
[2]Department of Physics, University of California at San Diego, La Jolla, CA 92903, USA

E-mail: `calmasan@kent.edu`

**Abstract.** Charge transport measurements under magnetic field and pressure on $Ce_{1-x}Yb_xCoIn_5$ single crystalline alloys revealed that: (i) relatively small Yb substitution suppresses the field induced quantum critical point, with a complete suppression for Yb doping $x > 0.07$; (ii) the superconducting transition temperature ($T_c$) and Kondo lattice coherence temperature ($T_{coh}$) decrease with $x$, yet they remain finite over the wide range of Yb concentrations; (iii) both $T_c$ and $T_{coh}$ increase with pressure; (iv) there are two contributions to resistivity, which show different temperature and pressure dependences, implying that both heavy and light quasiparticles contribute to inelastic scattering. We also analyzed the pressure dependence of both $T_{coh}$ and $T_c$ within the composite pairing theory. In the purely static limit, we find that the composite pairing mechanism necessarily causes opposite behaviors of $T_{coh}$ and $T_c$ with pressure: if $T_{coh}$ grows with pressure, $T_c$ must decrease with pressure and vice versa.

## 1. Introduction

Most of the current research efforts in unconventional superconductors are primarily focused on the understanding of their normal state properties, possible symmetries of the superconducting order parameter, as well as the microscopic mechanism of Cooper pairing. Generally, it is believed that superconductivity with $s$-wave symmetry of the order parameter is often realized in materials where electron-electron correlations are weak. In contrast, in materials with strong electronic correlations, the superconducting order parameter often develops nodes giving rise to $d$-wave or even $f$-wave pairing symmetries [1]. It is worth noting that unconventional superconductivity may develop from purely repulsive electron-electron interactions. Although a lot of progress has been made recently in our understanding of unconventional superconductivity in complex materials, the highly correlated nature of the many-body states makes the theoretical and experimental analysis of these materials very challenging.

The temperature-pressure ($T - P$) and temperature-doping ($T - x$) phase diagrams of most unconventional superconductors reveal an intricate interplay between magnetism and superconductivity [2, 3]. Namely, superconductivity emerges from an antiferromagnetic parent state upon doping with an excess of charge carriers, suggesting that the superconducting pairing mechanism could be related to the antiferromagnetic instability of the parent state. Moreover, superconductivity and antiferromagnetism coexist in most unconventional superconductors over a certain space of their $T - P$ and $T - x$ phase diagrams. Importantly, there is overwhelming evidence for an underlying quantum phase transition (QPT) at a quantum critical point (QCP)

separating magnetic and paramagnetic states within the superconducting phase, suggesting that strong magnetic fluctuations play a key role in the emergence of superconductivity.
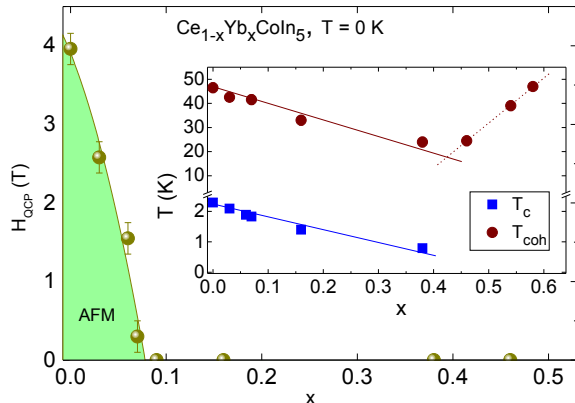


**Figure 1.** (Color online) Evolution of the field-induced quantum critical point $H_{QCP}$ of $Ce_{1-x}Yb_xCoIn_5$ as a function of Yb concentration $x$. Inset: $x$ dependence of the coherence temperature $T_{coh}$ and superconducting critical temperature $T_c$.

Although there are many examples where unconventional Cooper pairing is driven by the system's proximity to a magnetic QCP and is therefore mediated by an exchange of paramagnetic fluctuations, there are also a few notable exceptions. For instance, no signatures of magnetic fluctuations are found in the heavy-fermion superconductors $PuCoGa_5$ and $PuRhGa_5$ [4, 5, 6], most probably due to the mixed-valence state of the Pu ion. Similarly, the magnetic susceptibility of the recently discovered high-temperature heavy-fermion superconductor $Np_2Pd_5Al_2$ has a Curie-Weiss temperature dependence down to $T_c$, signaling the absence of pronounced magnetic interactions between the Np moments [7]. Intriguingly, although there are multiple evidences for the presence of strong magnetic fluctuations in $CeCoIn_5$ [8], superconductivity remains robust with respect to alloying this parent compound by Yb substitution on the Ce site [9]. This robustness of superconductivity against substitution-induced disorder points towards an alternative microscopic origin of superconductivity in this system.

In this paper, we focus on the the nature of the pairing mechanism and the issue of quantum criticality in $Ce_{1-x}Yb_xCoIn_5$ alloys. We also present a theoretical study of the pressure dependence of the Kondo lattice coherence and superconducting critical temperatures within the frame of the composite pairing theory.

## 2. Charge Transport

**General remarks.** The resistivity of $Ce_{1-x}Yb_xCoIn_5$ ($0.00 \leq x \leq 0.54$) alloys exhibits properties typical of heavy fermion systems [9, 10, 11], but our detailed analysis of charge transport measurements in the presence of magnetic field and hydrostatic pressure has revealed many interesting and unusual features that emerge with Yb doping. These results have allowed us to extract information about the evolution of the magnetic-field-tuned QCP present in $CeCoIn_5$ [12] with Yb doping and about the nature of the superconducting pairing.

At ambient pressure, the parent compound $CeCoIn_5$ of the $Ce_{1-x}R_xCoIn_5$ series (R is a rare earth) has been shown to be in close proximity to an antiferromagnetic QCP that is at an inaccessible negative pressure $P_c$ [13, 14]. With magnetic field ($H$) and $P$ as control parameters, thermal expansion [15] and current-voltage measurements in the mixed state [8] have revealed a quantum critical line in the $H$-$P$ plane of $CeCoIn_5$ at $T = 0$ K. In addition, magneto-transport measurements show that Kondo coherent scattering dominates the physics of $CeCoIn_5$ at relatively high temperatures [10, 11]. Substitutional disorder by alloying the $f$-electron sites with magnetic or non-magnetic rare earth ions has been employed as a tuning parameter. Irrespective of the magnetic nature of the substituent, the response of all these compounds is the same - the suppression of both superconducting transition temperature ($T_c$) and Kondo lattice coherence ($T_{coh}$) temperatures with substitutional disorder - with a full

suppression of $T_c$ at about 20% and $T_{coh}$ at around 40% of substitutional disorder [16].

**Experimental details.** Single crystals of $Ce_{1-x}Yb_xCoIn_5$ ($0 \leq x \leq 0.54$), where $x$ is the actual Yb doping, were grown using an indium self-flux method. The quality and structural details of the grown crystals were checked with X-ray powder diffraction and energy dispersive X-ray techniques. We note that the actual Yb doping differ from the nominal concentration and a detailed analysis of the relationship between actual and nominal doping has been discussed in Ref. [17].

The single crystals studied have a typical size of $1.0 \times 0.5 \times 0.1$ mm$^3$, with the c-axis along the shortest dimension of the crystals. The crystals were etched in concentrated HCl to remove the indium left on the surface during the growth process and were then rinsed thoroughly in ethanol. Four leads were attached to the single crystals, with the electrical current $I \parallel$ a-crystallographic axis. Charge transport measurements were performed for temperatures between 2 K and 300 K and hydrostatic pressures ($P$) up to 8.6 kbar.
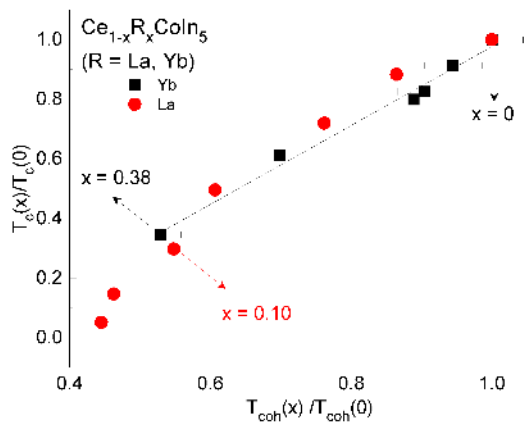


**Figure 2.** (Color online) Plot of superconducting critical temperature $T_c$ vs. Kondo lattice coherence temperature $T_{coh}$ normalized by the corresponding values of the undoped sample, for Yb and La [18] doping on Ce-site.

**Suppression of the field induced QCP.** Major deviations from standard behavior [16] are observed when the rare earth is in the intermediate-valence state as is Yb in $Ce_{1-x}Yb_xCoIn_5$ [9, 19]: superconductivity and Kondo coherence are weakly suppressed with Yb doping and extend to large Yb concentrations (inset to Fig. 1), in contrast with the behavior of all the other rare-earth substitutions discussed above, and, in addition, these alloys display a non-Fermi liquid (NFL) behavior for the whole Yb doping range [9, 10, 20]. The fact that $T_c$ and $T_{coh}$ are unusually robust to Yb substitution suggests that the strong pair-breaking effects of impurity substitution are reduced by the cooperative intermediate valence state of Yb [9, 19]. In fact, it has been proposed that there are strong impurity correlations between Yb ions at low Yb concentrations that result in a healing effect on $T_c$ and $T_{coh}$ [21]. On the other hand, the field-induced quantum critical point ($H_{QCP}$), which is finite for smaller Yb doping, is suppressed rapidly to almost zero at about 7% of Yb doping (Fig. 1), indicating that this doping is close to the critical value $x_c$, with a magnetic order for $x < x_c$ and paramagnetism for $x > x_c$. Recent penetration depth measurements suggest the appearance of a nodeless superconducting order parameter state at 20% nominal (7% actual) Yb doping [20]. The significant change in Fermi-surface topology revealed by these penetration depth and de Haas-van Alphen measurements [22] confirms that, indeed, the alloy with 7% Yb doping is quantum critical.

The rapid suppression of $H_{QCP}$ with Yb doping, along with the robustness of $T_{coh}$ and $T_c$ also suggests that spin fluctuations are not the "glue" for Cooper pairs. In addition, the scaling of the doping dependent $T_c$ and $T_{coh}$, normalized to the corresponding values for CeCoIn$_5$ (Fig. 2), shows that many-body coherence and superconductivity have the same microscopic origin: the hybridization between the conduction electrons with the localized Ce f-moments. The data for La substitution on the Ce site, also shown in Fig. 2, reveal that the same scaling works up to
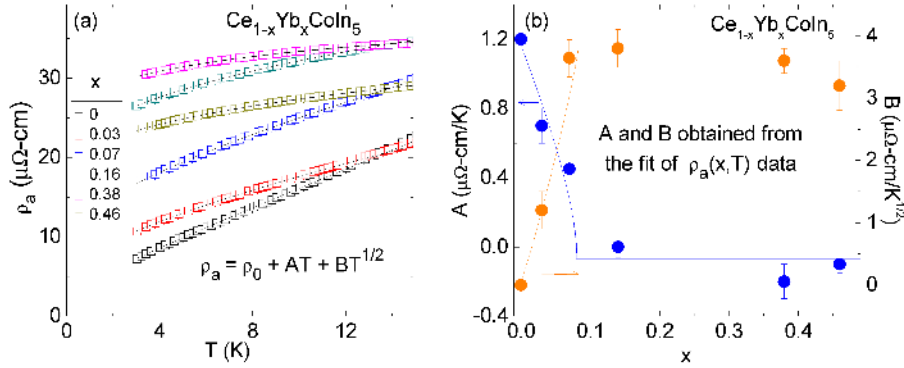
**Figure 3.** (Color online)(a) Fits of the resistivity data with $\rho_a = \rho_0 + AT + B\sqrt{T}$ for different doping levels of Yb in the temperature range 3 K $< T <$ 15 K. (b) Doping $x$ dependence of parameters $A$ and $B$ obtained from fits of the resistivity data shown in panel (a).

10% of La doping, which is an indication that the onset of many-body coherence in the Kondo lattice and the emergence of the superconductivity have the same physical origin in this system too.

**Temperature dependence of resistivity.** Another interesting phenomenon that is consistently observed in $Ce_{1-x}Yb_xCoIn_5$ alloys over the whole Yb doping range is the sublinear $T$ dependence of resistivity in the normal state, just above $T_c$ [9]. The presence of a NFL behavior is usually associated with the presence of a quantum phase transition tuned by the three control parameters: pressure, doping, or field. Nevertheless, as shown in Fig. 1, the magnetic order is fully suppressed for $x > x_c \approx 0.07$. Thus, the NFL behavior at higher Yb-doping can not be attributed to the presence of quantum spin fluctuations. With this in mind, we further investigated this puzzling NFL behavior through in plane resistivity ($\rho_a$) measurements. Our analysis has revealed that $\rho_a$ has a $\sqrt{T}$ dependence, except for the lower doping levels ($x \leq 0.07$) where it exhibits an additional linear-in-$T$ contribution; thus, we were able to fit all the data very well for $3 < T < 15$ K [see Fig. 3(a)] with

$$\rho_a(x,T) = \rho_0 + AT + B\sqrt{T}, \qquad (1)$$

where $\rho_0$, $A$, and $B$ are doping-dependent fitting parameters. Figure 3(b) shows $A$ and $B$ vs doping. A few features of this graph are worth noting. First, $A$ is non-zero, but it decreases rapidly with increasing $x$, and it becomes negligible for $x > 0.07$. We remind the reader that quantum spin fluctuations are present for $x < x_c \approx 0.07$ and absent for $x > x_c$. Thus, there is a direct correlation between the presence of the linear-in-$T$ contribution in resistivity and the presence of quantum spin fluctuations. In addition, there is a direct correlation between the suppression of $A$ and $H_{QCP}$ (see Fig. 1) with doping. At this point we do not understand its origin. Second, the $\sqrt{T}$ contribution to resistivity is absent for the stoichiometric parent compound, i.e., $B(x=0) = 0$. Furthermore, this contribution initially increases with increasing Yb concentration up to $x \approx 0.07$ and then it saturates for higher Yb doping. The microscopic origin of this behavior may be due to changes in the electronic structure of Yb: it has been shown that the Yb ions in the $Ce_{1-x}Yb_xCoIn_5$ alloys display an intermediate valence that decreases with increasing $x$ and saturates to a value of 2.3 for nominal $x \geq 0.20$ (actual $x \geq 0.07$) [19].

**Charge transport under pressure: heavy and light Fermi surfaces.** To further explore the origin of the NFL behavior in $Ce_{1-x}Yb_xCoIn_5$ alloys and the possibility of an alternative
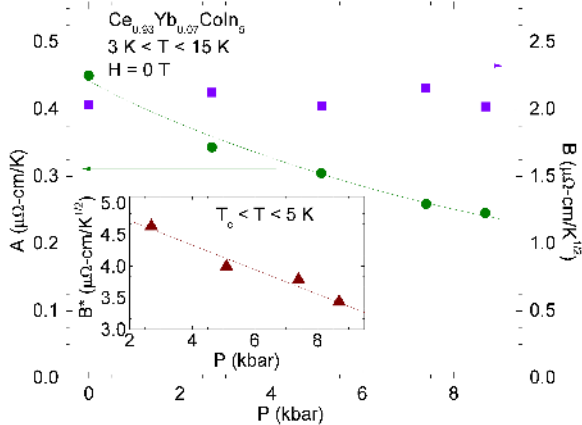
**Figure 4.** (Color online) Pressure $P$ dependence of parameters $A$ and $B$ obtained from the fits of the resistivity data for $Ce_{0.93}Yb_{0.07}CoIn_5$ with $\rho_a(P,T) = \rho_0 + AT + B\sqrt{T}$. The fitting is performed over the temperature range $3\ \mathrm{K} \leq T \leq 15\ \mathrm{K}$. Inset: $P$ dependence of parameter $B^*$ obtained from the fits of the resistivity data with $\rho_a(P,T) = \rho_0 + B^*\sqrt{T}$.
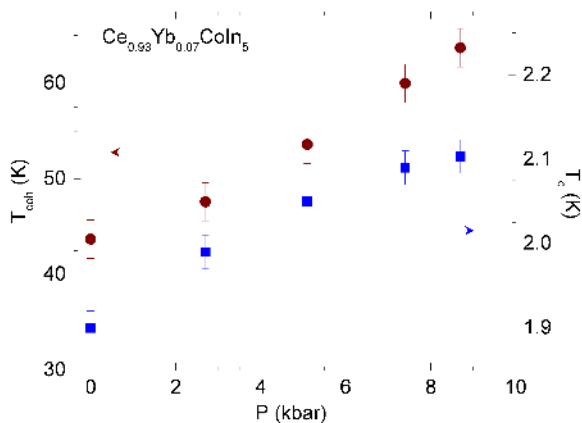


**Figure 5.** (Color online) Pressure $P$ dependence of coherence temperature $T_{\mathrm{coh}}$ and superconducting transition temperature $T_c$ for $Ce_{0.93}Yb_{0.07}CoIn_5$ for pressures up to 8.5 kbar.

pairing mechanism in this system, we performed resistivity measurements under hydrostatic pressure on the quantum critical alloy, i.e., on the $x = 0.07$ crystals. These measurements have revealed that the resistivity data are best fitted with $\rho_a(P,T) = \rho_0 + AT + B\sqrt{T}$ for $3\ \mathrm{K} < T < 15$ K and $\rho_a(P,T) = \rho_0 + B^*\sqrt{T}$ for $T_c < T < 5$ K. The main panel in Fig. 4 shows that $A$ decreases with increasing $P$, which is expected because it is attributed to quantum spin fluctuations, which are suppressed with pressure in Ce based heavy-fermion alloys [23, 24, 8, 25]. On the other hand, $B$ is insensitive to pressure. We have shown in Fig. 3(b) that the $\sqrt{T}$ contribution is absent in the parent compound $CeCoIn_5$, but it increases with increasing doping. This behavior, together with the fact that $B$ is independent of pressure, suggests that the origin of the $\sqrt{T}$ contribution for $3 < T < 15$ K is inelastic scattering of quasiparticles from the small Fermi surface. On the other hand, the absence of any linear-in-$T$ resistivity just above $T_c$ along with the decrease of $B^*$ with increasing $P$ (inset to Fig. 4) show that superconducting fluctuations dominate this $T$ region and that the inelastic scattering events leading to the $\sqrt{T}$ dependence in this temperature range involve quasiparticles from the heavy Fermi surface. Indeed, as Fig. 5 shows, both $T_{\mathrm{coh}}$ and $T_c$ increase with increasing pressure up to 8.5 kbar. This is expected within a weak-coupling theory of superconductivity [26] because $T_{\mathrm{coh}}$ sets a renormalized Fermi energy scale, so that

$$T_c \sim T_{\mathrm{coh}} \exp\left(-\frac{1}{\lambda_{SC}}\right), \tag{2}$$

where $\lambda_{SC}$ is a dimensionless coupling constant. For a small enough pressure $P$, we can neglect the pressure dependence of $\lambda_{SC}$ and it follows that $T_c(P) \propto T_{\mathrm{coh}}(P)$. In the limit of strong coupling superconductivity we still expect that $T_c(P) \propto T_{\mathrm{coh}}(P)$. Intriguingly, the robustness of $T_c$ on one hand, and its relative insensitivity to the value of the field-induced quantum critical

point $H_{\rm QCP}$, on the other hand, may indicate that a 'hidden' quantum critical point provides a pairing glue for the heavy-quasiparticles. A detailed discussion of this issue goes, however, beyond the scope of this paper.

In what follows, we demonstrate that the pressure dependence of $T_c$ and $T_{\rm coh}$ allows one to distinguish between various microscopic mechanisms for superconductivity. In particular, we show that our data in Fig. 5 are in fact inconsistent with the prediction of the composite pairing mechanism that suggests an increase in $T_{\rm coh}$ and a decrease in $T_c$ with increasing pressure.

### 3. Pressure Effects in Composite Pairing Superconductivity

Composite pairing theory has recently emerged as a prominent microscopic mechanism for superconducting pairing in heavy-fermion materials [27, 28, 29, 30]. At the heart of the theory is the idea that virtual fluctuations of an $f$-electron ion between magnetic (say $f^1$) and non-magnetic ($f^0$ and $f^2$) valence states become resonant [31] and, in principle, can promote superconducting pairing [27]. It is crucial that the emerging superconducting amplitude is anisotropic in momentum, signaling an onset of unconventional superconductivity. This in turn implies that the composite pairing can only be realized in the lattice of magnetic moments. It is also worth mentioning that, initially, the idea of the composite pairing has been developed in the context of odd-frequency Cooper pairing and its realization in heavy-fermion materials [32, 33, 34]. Subsequently, it was realized that even-frequency composite pairing can be regarded as an alternative to odd-frequency pairing with the order parameter given by the expectation value, which also contains a local spin operator [34].
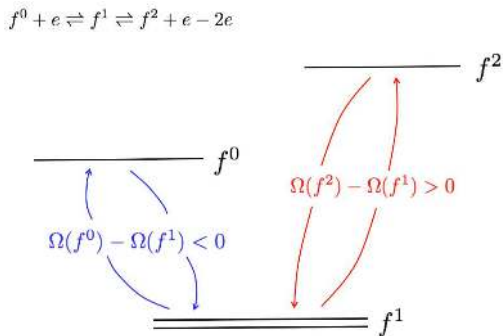


**Figure 6.** Schematic presentation for the virtual charge fluctuations between magnetic $f^1$ and non-magnetic valence configurations: $f^1 \rightleftharpoons f^0 + e$ via the first conduction channel and $f^1 \rightleftharpoons f^2 - e$ via the second conduction channel. Since the change in the ionic radius is opposite for the two channels, we expect the opposite behavior for the change in the corresponding coherence temperatures with pressure.

In this Section we theoretically study the effect of hydrostatic pressure on composite pairing. Specifically, we evaluate the pressure dependence of $T_{\rm coh}$ and $T_c$. For simplicity we will ignore the presence of disorder, so strictly speaking for the arguments presented below we assume the presence of a spatially homogeneous lattice. Our primary goal here is to show that the microscopic mechanism for the composite pairing necessarily implies opposite behaviors of $T_{\rm coh}$ and $T_c$ with pressure, which can be traced to the opposite changes in the ionic sizes as the resonance valence fluctuations take place.

#### 3.1. Model

We consider the two-channel Kondo lattice Hamiltonian, which is obtained from the Anderson lattice model by formally integrating out high-energy states by means of the Schrieffer-Wölff transformation [31, 27, 28]. We have:

$$H = \sum_{\mathbf{k}\sigma} \epsilon_{\mathbf{k}} c_{\mathbf{k}\sigma}^{\dagger} c_{\mathbf{k}\sigma} + \frac{1}{2} \sum_{\mathbf{k}\alpha,\mathbf{p}\beta} \sum_j J_{\mathbf{k},\mathbf{p}} c_{\mathbf{k}\alpha}^{\dagger} c_{\mathbf{p}\beta} \left( \vec{\sigma}_{\alpha\beta} \cdot \vec{S}_f(j) \right) e^{i(\mathbf{p}-\mathbf{k})\cdot\mathbf{R}_j}, \qquad (3)$$

where $c_{\mathbf{k}\sigma}^{\dagger}$ is a fermionic creation operator, $\mathbf{k}$ is a momentum, $\sigma = \uparrow, \downarrow$, $\epsilon_{\mathbf{k}} = -\frac{t}{4}(\cos k_x + \cos k_y) - \mu$, $t$ is a hopping amplitude, $\mu$ is a chemical potential, and $\vec{S}_f(j) = \frac{1}{2} f_{j\nu}^{\dagger} \vec{\sigma}_{\nu\eta} f_{j\eta}$, written using

the Abrikosov fermionic representation, accounts for the localized cerium $f$-moments at site $\vec{R}_j$. Note that, for simplicity, we choose the two-dimensional spectrum for the conduction electrons. The momentum dependent exchange couplings $J_{\mathbf{p},\mathbf{k}} = J_1\phi_{1\mathbf{k}}\phi_{2\mathbf{p}} + J_2\phi_{2\mathbf{k}}\phi_{2\mathbf{p}}$ include exchange couplings $J_{1,2} > 0$ for the electrons in the first and second conduction channels, while $\phi_{\Gamma\mathbf{k}}$ are the corresponding form-factors. Without loss of generality, we choose them in the following form $\phi_{1\mathbf{k}} = 1$ ($s$-wave) and $\phi_{2\mathbf{k}} = \cos k_x - \cos k_y$ ($d$-wave). The mean-field analysis of the model (3) shows that at $T_{\mathrm{coh}}$ the heavy-fermion state forms. Within the mean-field approximation, the formation of the heavy-fermion state is governed by the development of the non-zero expectation value $\langle c_{j\alpha}^\dagger f_{j\alpha}\rangle$ at each site. Interestingly, for $J_2 < J_1$ an anomalous expectation value can develop, signaling the onset of either a charge-density wave state or superconductivity. The proper choice of the phase stabilizes the superconducting state with a critical temperature [27] $T_c \sim T_{coh}\exp\left(-1/\nu_F J_2\right)$ where $\nu_F$ is the density of states at the chemical potential. This expression is reminiscent of the BCS weak-coupling expression for the critical temperature. As we will show below, $T_c$ shows a strong pressure dependence. Finally, we note that the mean-field theory results at ambient pressure are reproduced by various numerical approaches [35, 36, 34]. More importantly, the composite pairing mechanism for superconductivity can be extended to systems with mixed-valence [30]. However, to this date, the mean-field theory of the composite pairing state for the $f$-electron systems in the mixed-valence regime has not been numerically confirmed.

*3.2. Mean-field theory: effect of hydrostatic pressure*
The mean-field theory is formulated by performing the decoupling in the interacting part of the Hamiltonian (3). This is an approximation which becomes exact in the limit when the number of fermionic flavors $N$ goes to infinity. Therefore, to make our mean-field approximation controlled, we generalize our model from SU(2) to symplectic-$N$ [28] by replacing the Pauli spin operators $\boldsymbol{\sigma}_{\alpha\beta} \to (\boldsymbol{\sigma}_N)_{\alpha\beta}$. At ambient pressure we find:

$$\mathcal{F}_0 = -NT\sum_{\mathbf{k},\pm}\log[2\cosh(\beta\omega_{\mathbf{k}\pm}/2)] + N\mathcal{N}_s\sum_{\Gamma=1,2}\frac{v_\Gamma^2}{J_\Gamma}, \tag{4}$$

where $\beta = 1/k_B T$, $\mathcal{N}_s$ is a number of lattice sites, $v_{1,2}$ are corresponding mean-field amplitudes that describe the onset of coherence and superconductivity, while $\omega_{\mathbf{k}\pm}$ account for dispersion of newly formed electron bands $\omega_{\mathbf{k}\pm} = \sqrt{\alpha_{\mathbf{k}} \pm (\alpha_{\mathbf{k}}^2 - \gamma_{\mathbf{k}}^2)^{1/2}}$, where we have introduced functions $\alpha_{\mathbf{k}} = v_{\mathbf{k}+}^2 + \frac{1}{2}\left(\epsilon_{\mathbf{k}}^2 + \lambda^2\right)$, $\gamma_{\mathbf{k}}^2 = (\epsilon_{\mathbf{k}}\lambda - v_{\mathbf{k}-}^2)^2 + 4(v_{1\mathbf{k}}v_{2\mathbf{k}})^2$, $v_{1\mathbf{k}} = v_1\phi_{1\mathbf{k}}$, $v_{2\mathbf{k}} = v_2\phi_{2\mathbf{k}}$, and $v_{\mathbf{k}\pm}^2 = v_{1\mathbf{k}}^2 \pm v_{2\mathbf{k}}^2$.
For the Ce ions, the change in the $f$-shell occupation is positive due to its electronic nature, so that the leading resonance scattering involves conduction electrons in the first channel and a zero-energy boson with amplitude $v_1$, and an electron: $f^1(j,m) \rightleftharpoons f^0(j,m) + e$. In contrast, the resonance scattering in the second conduction channel involves a zero energy boson with an amplitude $v_2$ and a hole: $f^1(j,m) \rightleftharpoons f^2(j,m) + e - 2e$. When resonance develops in both channels, for the total volume of the system within the mean-field theory, we write: [37]

$$\Omega_t = \Omega(f^0)v_1^2 + (1 - v_1^2 - v_2^2)\Omega(f^1) + \Omega(f^2)v_2^2, \tag{5}$$

where $\Omega(f^n)$ are the cell volumes for the singlet ($n = 0, 2$) states and a doublet ($n = 1$) state. It is convenient to introduce the change in the cell volumes: $\delta\Omega_{1\mathrm{ch}} = \Omega(f^0) - \Omega(f^1)$ is negative and accounts for the difference in cell volumes between two $f$-ion configurations for the resonance in the first channel. Similarly, $\delta\Omega_{2\mathrm{ch}} = \Omega(f^2) - \Omega(f^1)$ is positive and yields the difference in
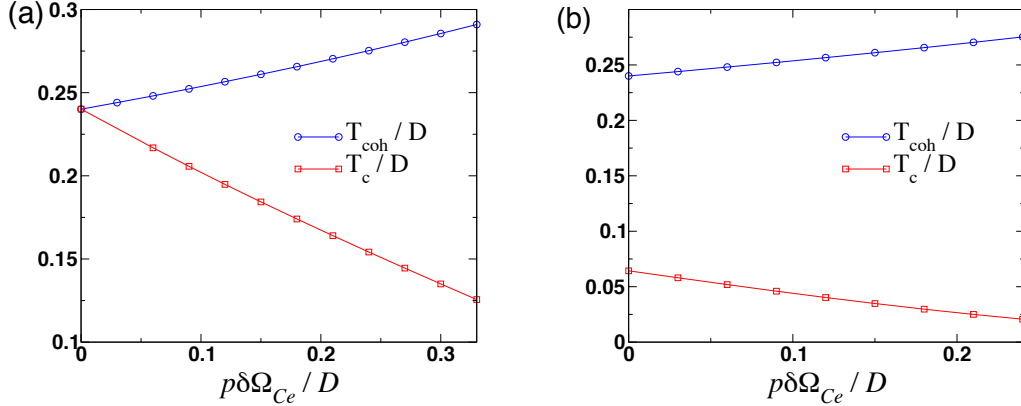
**Figure 7.** (Color online) Plots of the pressure dependence of the Kondo lattice coherence temperature $T_{\mathrm{coh}}$ and superconducting critical temperature $T_c$ from the solution of the mean-field theory for the two-channel Kondo lattice model. The first screening channel corresponds to the fluctuations between $f^1$ and $f^0$ cerium valence states, so that the change in the ionic volume is negative $\delta\Omega_{\mathrm{1ch}} = \Omega(f^0) - \Omega(f^1) < 0$. The amplitude $v_1$ becomes non-zero at $T = T_{\mathrm{coh}}$ as the resonance $f^1 \rightleftharpoons f^0 + e$ develops. Similarly, the superconductivity is driven by the hybridization of the conduction electrons with the $f$-states in the second channel corresponding to the fluctuations between $f^1$ and doubly occupied singlet $f^2$: $f^1 \rightleftharpoons f^2 + e - 2e$. Since the $f^2$ state has a larger ionic volume $\delta\Omega_{\mathrm{2ch}} = \Omega(f^2) - \Omega(f^1) > 0$. Here we define $\delta\Omega_{Ce} = -\delta\Omega_{\mathrm{1ch}} = \delta\Omega_{\mathrm{2ch}}$. We use the following set of parameters: $\mu = -0.125t$, $D = t$ and $J_1 = 0.5t$. Panel (a): $J_2 = 1.05J_1$. Panel (b): $J_2 = 0.7J_1$.

volume between ionic configurations for the resonance in the second channel, Fig. 6. In what follows, we assume that $\delta\Omega_{\mathrm{2ch}} \approx -\delta\Omega_{\mathrm{1ch}} = \delta\Omega_{\mathrm{Ce}}$. For the free energy we find:

$$\mathcal{F} = \mathcal{F}_0 + P\Omega_t. \tag{6}$$

The mean-field equations are obtained by minimizing the free energy $\mathcal{F} = \mathcal{F}_0 + p\Omega_t$ with respect to $\lambda$ and $(v_\Gamma)^2$ ($\Gamma = 1, 2$). This yields:

$$\frac{1}{\mathcal{N}_s} \sum_{\mathbf{k}\pm} \frac{\tanh(\omega_{\mathbf{k}\pm}/2T)}{2\omega_{\mathbf{k}\pm}} \left( \lambda \pm \frac{\lambda\alpha_{\mathbf{k}} - \epsilon_{\mathbf{k}}(\epsilon_{\mathbf{k}}\lambda - v_{\mathbf{k}-}^2)}{\sqrt{\alpha_{\mathbf{k}}^2 - \gamma_{\mathbf{k}}^2}} \right) = 0,$$

$$\frac{1}{\mathcal{N}_s} \sum_{\mathbf{k}\pm} \phi_{1\mathbf{k}}^2 \frac{\tanh(\omega_{\mathbf{k}\pm}/2T)}{2\omega_{\mathbf{k}\pm}} \left( 2 \pm \frac{(\epsilon_{\mathbf{k}} + \lambda)^2}{\sqrt{\alpha_{\mathbf{k}}^2 - \gamma_{\mathbf{k}}^2}} \right) = \frac{4}{J_1} + 4P\delta\Omega_{\mathrm{1ch}}, \tag{7}$$

$$\frac{1}{\mathcal{N}_s} \sum_{\mathbf{k}\pm} \phi_{2\mathbf{k}}^2 \frac{\tanh(\omega_{\mathbf{k}\pm}/2T)}{2\omega_{\mathbf{k}\pm}} \left( 2 \pm \frac{(\epsilon_{\mathbf{k}} - \lambda)^2}{\sqrt{\alpha_{\mathbf{k}}^2 - \gamma_{\mathbf{k}}^2}} \right) = \frac{4}{J_2} + 4P\delta\Omega_{\mathrm{2ch}}.$$

In the normal phase either $v_1$ or $v_2$ is nonzero, corresponding to the development of the Kondo effect in the strongest channel. Here we will consider two cases: the first one corresponds to the choice of $J_1/J_2$ such that resonances in both channels develop simultaneously, while in the second case the condensation occurs in the first channel. From the mean-field equations (7) we can already see that the pressure has an opposite effect on the condensation temperatures in two channels: since $\delta\Omega_{\mathrm{1ch}} < 0$ it means that the effective exchange coupling $\tilde{J}_1(P) > J_1(P = 0)$, signaling an increase of the Kondo lattice coherence temperature. In contrast, $\tilde{J}_2(P) < J_2(P = 0)$, implying a decrease in $T_c$ with pressure. We compute the corresponding dependences of $T_c$

and $T_{\mathrm{coh}}$ on pressure by solving Eqs. (7) numerically. The results are shown on Fig. 7. We note also that while opposite tendencies in $T_{\mathrm{coh}}$ and $T_c$ in response to pressure appears to be a universal feature for the composite pairing mechanism, the rates with which $T_{\mathrm{coh}}$ and $T_c$ change with pressure are not universal and depend on the microscopic features of the model.

## 4. Summary

Our findings on the $\mathrm{Ce}_{1-x}\mathrm{Yb}_x\mathrm{CoIn}_5$ system are in line with the emerging scenario of two coexisting electronic networks (one of Ce $f$-moments and another of Yb $f$-electrons in an intermediate valence state) coupled to the conduction electrons. This is consistent with our observation that the quantum fluctuations are suppressed for $x = 0.07$ Yb doping (see $H_{QCP}$ in Fig. 1) but $T_c$ stays robust suggesting that spin fluctuations could not be the glue for SC pairing. Furthermore, the robust nature of $T_{\mathrm{coh}}$ and $T_c$ and their scaling suggest that the emergence of SC and the onset of many-body coherence in the Kondo lattice have the same physical origin: hybridization between conduction and localized Ce $f$-electron states.

We have established that within the mean-field theory approach for the composite pairing scenario, $T_c$ decreases while $T_{\mathrm{coh}}$ increases with increasing $P$. These results are at odds with the experimental data in $\mathrm{Ce}_{1-x}\mathrm{Yb}_x\mathrm{CoIn}_5$, which show that both $T_{\mathrm{coh}}$ and $T_c$ initially increase with pressure (Fig. 5). By examining $T_c \sim T_{\mathrm{coh}} \exp\left(-1/\nu_F J_2\right)$ we see that one possible way to reconcile the composite pairing theory [29, 38] with the experimental data would be to assume that quantum valence fluctuations may effectively renormalize the spin exchange coupling $J_2$ to compensate for the effect caused by the change in the ionic volume. In this case, only $T_{\mathrm{coh}}(P)$ will have a pronounced pressure dependence and $T_c(P) \sim T_{\mathrm{coh}}(P)$, in agreement with experimental observations. However, a detailed study of this problem clearly goes beyond the scope of this paper and will be addressed elsewhere.

## References

[1] Norman M R 2011 *Science* **332** 196–200
[2] Pfleiderer C 2009 *Rev. Mod. Phys.* **81**(4) 1551–1624
[3] Scalapino D J 2012 *Rev. Mod. Phys.* **84**(4) 1383–1417
[4] Curro N, Caldwell T, Bauer E, Morales L, Graf M, Bang Y, Balatsky A, Thompson J and Sarrao J 2005 *Nature* **434** 622–625
[5] Sakai H, Tokunaga Y, Fujimoto T, Kambe S, Walstedt R E, Yasuoka H, Aoki D, Homma Y, Yamamoto E, Nakamura A, Shiokawa Y, Nakajima K, Arai Y, Matsuda T D, Haga Y and Ōnuki Y 2005 *Journal of the Physical Society of Japan* **74** 1710–1713
[6] Bauer E D, Altarawneh M M, Tobash P H, Gofryk K, Ayala-Valenzuela O E, Mitchell J N, McDonald R D, Mielke C H, Ronning F, Griveau J C, Colineau E, Eloirdi R, Caciuffo R, Scott B L, Janka O, Kauzlarich S M and Thompson J D 2012 *Journal of Physics: Condensed Matter* **24** 052206
[7] Aoki D, Haga Y, Matsuda T D, Tateiwa N, Ikeda S, Homma Y, Sakai H, Shiokawa Y, Yamamoto E, Nakamura A, Settai R and Ōnuki Y 2007 *Journal of the Physical Society of Japan* **76** 063701
[8] Hu T, Xiao H, Sayles T A, Dzero M, Maple M B and Almasan C C 2012 *Phys. Rev. Lett.* **108**(5) 056401
[9] Shu L, Baumbach R E, Janoschek M, Gonzales E, Huang K, Sayles T A, Paglione J, O'Brien J, Hamlin J J, Zocco D A, Ho P C, McElroy C A and Maple M B 2011 *Phys. Rev. Lett.* **106**(15) 156403
[10] Hu T, Singh Y P, Shu L, Janoschek M, Dzero M, Maple M B and Almasan C C 2013 *Proceedings of the National Academy of Sciences* **110** 7160–7164
[11] Singh Y P, Haney D J, Huang X Y, Lum I K, White B D, Dzero M, Maple M B and Almasan C C 2014 *Phys. Rev. B* **89**(11) 115106
[12] Paglione J, Tanatar M A, Hawthorn D G, Boaknin E, Hill R W, Ronning F, Sutherland M, Taillefer L, Petrovic C and Canfield P C 2003 *Phys. Rev. Lett.* **91**(24) 246405

[13] Sidorov V A, Nicklas M, Pagliuso P G, Sarrao J L, Bang Y, Balatsky A V and Thompson J D 2002 *Phys. Rev. Lett.* **89**(15) 157004

[14] Nair S, Stockert O, Witte U, Nicklas M, Schedler R, Kiefer K, Thompson J D, Bianchi A D, Fisk Z, Wirth S and Steglich F 2010 *Proceedings of the National Academy of Sciences*

[15] Zaum S, Grube K, Schäfer R, Bauer E D, Thompson J D and v Löhneysen H 2011 *Phys. Rev. Lett.* **106**(8) 087003

[16] Paglione J, Sayles T A, Ho P C, Jeffries J R and Maple M B 2007 *Nat. Phys.* **3** 703–706

[17] Jang S, White B, Lum I, Kim H, Tanatar M, Straszheim W, Prozorov R, Keiber T, Bridges F, Shu L, Baumbach R, Janoschek M and Maple M 2014 *Philosophical Magazine* **94** 4219–4231

[18] Petrovic C, Budko S, Kogan V and Canfield P 2002 *Physical Review B* **66** 054534

[19] Dudy L, Denlinger J D, Shu L, Janoschek M, Allen J W and Maple M B 2013 *Phys. Rev. B* **88**(16) 165118

[20] Kim H, Tanatar M A, Flint R, Petrovic C, Hu R, White B D, Lum I K, Maple M B and Prozorov R 2014 *arXiv:1404.3700v1*

[21] Dzero M and Huang X 2012 *Journal of Physics: Condensed Matter* **24** 075603

[22] Polyakov A, Ignatchik O, Bergk B, Götze K, Bianchi A D, Blackburn S, Prévost B, Seyfarth G, Côté M, Hurt D, Capan C, Fisk Z, Goodrich R G, Sheikin I, Richter M and Wosnitza J 2012 *Phys. Rev. B* **85**(24) 245119

[23] Jaccard D, Behnia K and Sierro J 1992 *Physics Letters A* **163** 475 – 480 ISSN 0375-9601

[24] Grosche F, Julian S, Mathur N and Lonzarich G 1996 *Physica B: Condensed Matter* **223** 50 – 52 ISSN 0921-4526 proceedings of the International Conference on Strongly Correlated Electron Systems

[25] Singh Y P, Haney D J, Huang X, Maple M B, Dzero M and Almasan C C 2014 *arXiv:1411.2524v1*

[26] Dzero M and Gor'kov L P 2004 *Phys. Rev. B* **69**(9) 092501

[27] Coleman P, Tsvelik A M, Andrei N and Kee H Y 1999 *Phys. Rev. B* **60**(5) 3608–3628

[28] Flint R, Dzero M and Coleman P 2008 *Nat Phys* **4** 643–648

[29] Flint R and Coleman P 2010 *Phys. Rev. Lett.* **105**(24) 246404

[30] Flint R, Nevidomskyy A H and Coleman P 2011 *Phys. Rev. B* **84**(6) 064514

[31] Kim T S and Cox D L 1997 *Phys. Rev. B* **55**(18) 12594–12619

[32] Coleman P, Miranda E and Tsvelik A 1993 *Phys. Rev. Lett.* **70**(19) 2960–2963

[33] Coleman P, Miranda E and Tsvelik A 1994 *Phys. Rev. B* **49**(13) 8955–8982

[34] Hoshino S and Kuramoto Y 2014 *Phys. Rev. Lett.* **112**(16) 167204

[35] Anders F B 2002 *Phys. Rev. B* **66**(2) 020504

[36] Anders F 2002 *The European Physical Journal B - Condensed Matter and Complex Systems* **28** 9–28 ISSN 1434-6028

[37] Zhang S 2002 *Phys. Rev. B* **65**(6) 064407

[38] Erten O, Flint R and Coleman P 2014 *arXiv:1402.7361v2*